Ethylene and Alkyne Carbon−Carbon Bond Cleavage across Tungsten−Tungsten Multiple Bonds

Rebecca L. M. Chamberlin,† Devon C. Rosenfeld, Peter T. Wolczanski,* and Emil B. Lobkovsky

Department of Chemistry & Chemical Biology, Baker Laboratory, Cornell University, Ithaca, New York 14853

Received January 17, 2002

Treatment of $[(silox)_2WH]_2$ (**1**) with RC≡CR′ (R = R′ = H, CH_3; R = H, R′ = Ph) afforded thermally unstable $[(silox)_2W]_2(\mu:\eta^2,\eta^2\text{-RCCR}')(\mu\text{-H})_2$ (R = R′ = H, **2a**; CH_3, **2b**; R = H, R′ = Ph, **2c**), which lose H_2 and convert to $[(silox)_2W]_2(\mu\text{-CR})(\mu\text{-CR}')$ (R = R′ = H, **4a**; CH_3, **4b**; R = H, R′ = Ph, **4c**). An X-ray structural study of **4b** revealed a nearly square W_2C_2 core and a *d*(WW) of 2.720(2) Å. Thermal degradation of $[(silox)_2W(CH_2CH_3)]_2$ (**5**) also produced **4b**, and with 2 equiv of C_2H_4, its formation is nearly quantitative with 2 equiv of EtH as a byproduct. Na/Hg reduction of $(silox)_2ClW{\equiv}WCl(silox)_2$ (**3**) in the presence of excess 2-butyne afforded $[(silox)_2W]_2(\mu:\eta^2,\eta^2\text{-MeC}_2\text{Me})$ (**8**), which could be treated with H_2 to give **2b** or thermolyzed to **4b**. A similar reduction of **3** with excess ethylene present afforded **4a** via $[(silox)_2W]_2(\mu\text{-CH})(\mu\text{-CH}_2)(\text{H})$ (**9**, −78 °C) followed by H_2 loss; ethylene cleavage does not proceed via **2a** or **8**. Related cleavage chemistry was not observed for $[(silox)_2TaH_2]_2$ (**10**) and excess ethylene, which formed $[(silox)_2HTaEt]_2$ (**11**) and, ultimately, $[(silox)_2EtTa](\mu\text{-CHCH}_2)(\mu\text{-H})_2[Ta(silox)_2]$ (**12**) and EtH. An X-ray structural study of **12** confirmed its configuration. Spectroscopic features of the molecules are addressed, and plausible mechanisms of carbon−carbon bond cleavage—whose thermodynamic impetus is the formation of μ-CR bridges—are discussed.

Introduction

The remarkable reactivity of the d^3−d^3 triple bond toward small-molecule substrates[1] is readily apparent in the interactions of alkynes with $(W{\equiv}W)^{6+}$-based complexes. Alkyne cleavage was originally[2] observed in the treatment of $(^tBuO)_3W{\equiv}W(O^tBu)_3$ with a variety of alkynes,[3] and alkylidyne products were isolated as pseudo-tetrahedral species or as Lewis-base adducts.[2−6] The immediate application of alkylidynes toward alkyne metathesis[7,8] was exploited, and the mechanistic evaluation of the alkyne scission process provided the connection between $\mu:\eta^2,\eta^2$-alkyne precursors and various cleavage products.[9,10] A fascinating array of alkyne adducts[10−21] and alkyne-coupling reactions[13−21] were discovered as extensive ligand and substrate surveys were conducted to determine the scope of the RCCR′ chemistry. In several instances[16−18] and in related studies,[19−28] formation of stable $W_2(\mu\text{-CR})$ functionalities was unavoidable and apparently irreversible.

In entering the area via the synthesis of $(silox)_2XW{\equiv}WX(silox)_2$ (X = Cl, H, Me, Et; silox = $^tBu_3SiO$),[29,30] steric features of the $^tBu_3Si$ group[31] were considered as potentially aiding alkyne or nitrile[2,32−34] and metal−metal bond cleavage to afford $(silox)_2XW{\equiv}CR$. As reported below, no alkyne reactivity was evident for X = Cl, Me, or Et, and hydride proved too small to avert the generation of dinuclear complexes. Nonetheless, subtle differences in reactivity were observed as a consequence of the silox ligand, including CH and CC bond activations and ethylene cleavage by the ditungsten linkages. Olefin cleavages and degradations of related alkyl

† Current address: Los Alamos National Laboratory, C-INC, MS J514, Los Alamos, NM 87545.

(1) (a) Chisholm, M. H. *J. Chem. Soc., Dalton Trans.* **1996**, 1781−1791. (b) Chisholm, M. H. *J. Organomet. Chem.* **1990**, *400*, 235−253. (c) Chisholm, M. H. *Acc. Chem. Res.* **1990**, *23*, 419−425. (d) Buhro, W. E.; Chisholm, M. H. *Adv. Organomet. Chem.* **1987**, *27*, 311−369. (e) Chisholm, M. H.; Conroy, B. K.; Eichhorn, B. W.; Folting, K.; Hoffman, D. M.; Huffman, J. C.; Marchant, N. S. *Polyhedron* **1987**, *6*, 783−792. (f) Chisholm, M. H.; Hoffman, D. M.; Huffman, J. C. *Chem. Soc. Rev.* **1985**, *14*, 69−91.

(2) Schrock, R. R.; Listemann, M. L.; Sturgeoff, L. G. *J. Am. Chem. Soc.* **1982**, *104*, 4291−4293.

(3) Listemann, M. L.; Schrock, R. R. *Organometallics* **1985**, *4*, 74−83.

(4) Chisholm, M. H.; Hoffman, D. M.; Huffman, J. C. *Inorg. Chem.* **1983**, *22*, 2903−2906.

(5) Freudenberger, J. H.; Pedersen, S. F.; Schrock, R. R. *Bull. Soc. Chim. Fr.* **1985**, 349−352.

(6) Cotton, F. A.; Schwotzer, W.; Shamshoum, E. S. *Organometallics* **1984**, *3*, 1770−1771.

(7) (a) Schrock, R. R. *J. Chem. Soc., Dalton Trans.* **2001**, 2541−2550. (b) Schrock, R. R. *Acc. Chem. Res.* **1986**, *19*, 342−348.

(8) (a) Wengrovius, J. H.; Sancho, J.; Schrock, R. R. *J. Am. Chem. Soc.* **1981**, *103*, 3932−3934. (b) Sancho, J.; Schrock, R. R. *J. Mol. Catal.* **1982**, *15*, 75−79.

(9) Chisholm, M. H.; Folting, K.; Hoffman, D. M.; Huffman, J. C. *J. Am. Chem. Soc.* **1984**, *106*, 6794−6805.

(10) Chisholm, M. H.; Conroy, B. K.; Huffman, J. C.; Marchant, N. S. *Angew. Chem., Int. Ed. Engl.* **1986**, *25*, 446−447.

(11) (a) Chisholm, M. H.; Folting, K.; Huffman, J. C.; Rothwell, I. P. *J. Am. Chem. Soc.* **1982**, *104*, 4389−4399. (b) Chisholm, M. H.; Conroy, B. K.; Folting, K.; Hoffman, D. M.; Huffman, J. C. *Organometallics* **1986**, *5*, 2457−2465.

(12) Chisholm, M. H.; Conroy, B. K.; Clark, D. L.; Huffman, J. C. *Polyhedron* **1988**, *7*, 903−918.

(13) Chisholm, M. H.; Cook, C. M.; Huffman, J. C.; Streib, W. E. *J. Chem. Soc., Dalton Trans.* **1991**, 929−937.

(14) Chisholm, M. H.; Lynn, M. A. *J. Organomet. Chem.* **1998**, *550*, 141−150.

(15) Chisholm, M. H.; Hoffman, D. M.; Huffman, J. C. *J. Am. Chem. Soc.* **1984**, *106*, 6806−6815.

10.1021/om020037n CCC: $22.00
Publication on Web 05/24/2002

complexes support the contention of extremely stable $W_2(\mu$-CR) linkages.

Results

Synthesis, Characterization, and Reactivity Studies. 1. Alkyne Adducts of [(silox)$_2$WH]$_2$. Treatment of [(silox)$_2$WH]$_2$ (**1**)[30] with RC≡CR′ (R = R′ = H, CH_3; R = H, R′ = Ph) afforded thermally unstable μ:η^2,η^2-adducts, [(silox)$_2$W]$_2$(μ:η^2,η^2-RCCR′)(μ-H)$_2$ (R = R′ = H, **2a** (−78 °C, minutes, hexanes); CH_3, **2b** (25 °C, 4 h, C_6D_6); R = H, R′ = Ph, **2c** (25 °C, 8h, C_6D_6)) in >90% yield as monitored by ^{1}H NMR spectroscopy (eq 1). In

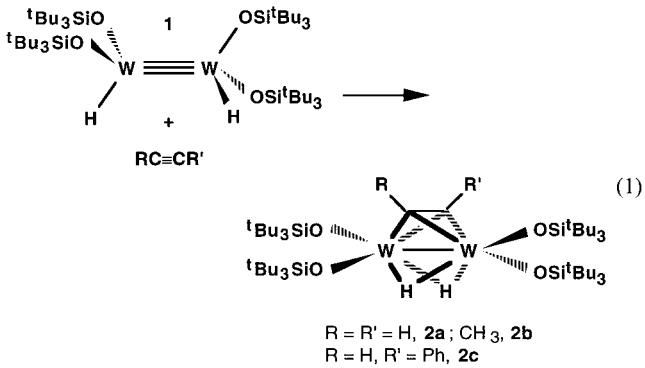

(1)

contrast, (silox)$_2$XW≡WX(silox)$_2$ (X = Cl (**3**), Me, Et) failed to react with acetylene or 2-butyne at room temperature. After extended thermolysis (100 °C) with excess acetylene, most of the starting material remained along with a copious blue-black precipitate assumed to be polyacetylene.[13] The formation of ditungsten alkyne adducts of **1** in the absence of additional donor ligands, and without further aggregation, is a testament to the steric bulk of the silox ligand. Steric factors are also reflected in the above reaction times, and larger alkynes such as diphenylacetylene and *tert*-butylacetylene failed to bind to **1** at 25 °C; higher temperatures gave complicated reaction mixtures.

The spectral features of the parent acetylene adduct, **2a**, are typical of the series (Table 1). Diastereotopic silox ligands, a single μ-acetylene CH resonance at δ 11.73, and equivalent hydride ligands resonating at δ 4.83 reflect molecular C_2 symmetry. Asymmetric bridging hydrides are implicated by two sets of ^{183}W satellites; J_{WH} = 39 and 176 Hz. The μ:η^2,η^2-acetylene carbons resonate as a doublet at δ 181.40 in the ^{13}C NMR spectrum, with a large J_{CH} value of 182 Hz, which is typical of structurally characterized, perpendicular acetylene adducts.[9] As expected, no tungsten coupling to the acetylene proton is observed ($J_{WH} \approx 0$), yet the corresponding J_{CW} of 115 Hz is relatively large. ^{1}H and ^{13}C shifts of **2a** appear downfield compared to related hexaalkoxide complexes[9] that contain additional ligands, perhaps reflecting the lower coordination number and corresponding lesser electron density at the tungsten centers (Table 2).

The 2-butyne adduct, **2b**, possesses spectral features remarkably similar to the parent species, with hydrides again resonating at δ 4.83 (J_{WH} = 42, 174 Hz) in the ^{1}H NMR spectrum. Diastereotopic silox ligands and a single methyl resonance at δ 3.41 indicate a close structural parallel with **2a**. Deuterium substitution into the hydride positions of **2b** permitted identification of a bridging W_2(H/D) stretch at 1522/1145 cm^{-1}.

The terminal phenyl acetylene derivative, **2c**, exhibits inequivalent silox and hydride resonances in the ^{1}H NMR spectrum as the symmetry is lowered from C_2. One hydride at δ 5.27 has tungsten satellites of 39 and 174 Hz, and its small J_{HH} of 3 Hz to the μ-acetylenic proton at δ 11.95 suggests the two groups are proximate. The other hydride at δ 5.22 is coupled only to tungsten (J_{WH} = 40, 165 Hz) and is presumed to lie on the side of the phenyl substituent. The average J_{WH} for each hydride in **2a**−**c** is 106.7(21) Hz, a value remarkably close to that of D_{2d} [(silox)$_2$W]$_2$(μ-H)$_4$, whose J_{WH} = 108 Hz was tentatively assigned to four symmetric, bridging hydrides.[30]

2. Alkyne Scission. Thermolysis of [(silox)$_2$W]$_2$(μ:η^2,η^2-C_2H_2)(μ-H)$_2$ (**2a**) at 80 °C for ∼5 h liberated dihydrogen and produced [(silox)$_2$W]$_2$(μ-CH)$_2$ (**4a**, eq 2), which was isolated as a fluffy yellow solid in 66% yield.

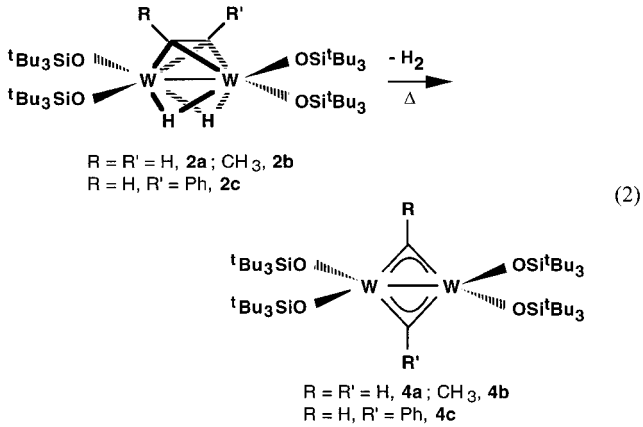

(2)

Its solubility in hydrocarbon and ethereal solvents was low at 25 °C but significant at 80 °C. The ^{1}H NMR

(16) Chisholm, M. H.; Eichhorn, B. W.; Folting, K.; Huffman, J. C. *Organometallics* **1989**, *8*, 49−66.
(17) Chisholm, M. H.; Eichhorn, B. W.; Huffman, J. C. *Organometallics* **1989**, *8*, 67−79.
(18) Chisholm, M. H.; Eichhorn, B. W.; Huffman, J. C. *Organometallics* **1989**, *8*, 80−89.
(19) Chisholm, M. H.; Hoffman, D. M.; Northius, J. M.; Huffman, J. C. *Polyhedron* **1997**, *16*, 839−847.
(20) Chisholm, M. H.; Folting, K.; Lynn, M. A.; Streib, W. E.; Tiedtke, D. B. *Angew. Chem., Int. Ed. Engl.* **1997**, *36*, 52−54.
(21) Chisholm, M. H.; Cook, C. M.; Huffman, J. C.; Streib, W. E. *Organometallics* **1993**, *12*, 2677−2685.
(22) Anderson, R. A.; Gayler, A. L.; Wilkinson, G. *Angew. Chem., Int. Ed. Engl.* **1976**, *15*, 609.
(23) Chisholm, M. H.; Cotton, F. A.; Extine, M.; Stults, B. R. *Inorg. Chem.* **1978**, *17*, 696−698.
(24) Liu, A. H.; Murray, R. C.; Dewan, J. C.; Santarsiero, B. D.; Schrock, R. R. *J. Am. Chem. Soc.* **1987**, *109*, 4282−4291.
(25) Chisholm, M. H.; Heppert, J. A.; Kober, E. M.; Lichtenberger, D. L. *Organometallics* **1987**, *6*, 1065−1073.
(26) Chisholm, M. H.; Heppert, J. A.; Huffman, J. C.; Thornton, P. *J. Chem. Soc., Chem. Commun.* **1985**, 1466−1467.
(27) Chisholm, M. H.; Heppert, J. A. *Adv. Organomet. Chem.* **1986**, *26*, 97−124.
(28) Chisholm, M. H.; Jansen, R. M.; Huffman, J. C. *Organometallics* **1992**, *11*, 2305−2307.
(29) Miller, R. L.; Wolczanski, P. T.; Rheingold, A. L. *J. Am. Chem. Soc.* **1993**, *115*, 10422−10423.
(30) Miller, R. L.; Lawler, K. A.; Bennett, J. L.; Wolczanski, P. T. *Inorg. Chem.* **1996**, *35*, 3242−3253.
(31) Wolczanski, P. T. *Polyhedron* **1995**, *14*, 3335−3362.
(32) Chisholm, M. H.; Folting, K.; Lynn, M. L.; Tiedtke, D. B.; Lemoigno, F.; Eisenstein, O. *Chem. Eur. J.* **1999**, *5*, 2318−2326.
(33) Chisholm, M. H.; Folting-Streib, K.; Tiedtke, D. B.; Lemoigno, F.; Eisenstein, O. *Angew. Chem., Int. Ed. Engl.* **1995**, *34*, 110−112.
(34) Chisholm, M. H.; Folting, K.; Huffman, J. C.; Lucas, E. A. *Organometallics* **1991**, *10*, 535−537.

Table 1. ^{1}H, ^{13}C, and ^{13}C{^{1}H} NMR Spectral Data (δ, assgmt, mult, J(Hz))[a] for Ditungsten and Ditantalum Derivatives in C_6D_6 unless Otherwise Noted

	^{1}H NMR (δ, mult, assgmt, J(Hz))		^{13}C{^{1}H} NMR (δ, assgmt, J(Hz))		
compound	$((H_3C)_3C)_3$	H/R	$C(CH_3)_3$	$C(CH_3)_3$	R
$[(silox)_2W]_2(\mu:\eta^2,\eta^2\text{-}C_2H_2)(\mu\text{-}H)_2$ (**2a**)	1.08	4.83, J_{WH} = 39, 176	30.49	23.62	181.40, J_{CH} = 182, J_{WC} = 115[b]
	1.36	11.73 (C_2H_2)	30.79	23.98	
$[(silox)_2W]_2(\mu:\eta^2,\eta^2\text{-}C_2Me_2)(\mu\text{-}H)_2$ (**2b**)	1.10	4.83, J_{WH} = 42, 174	30.64	23.21	22.39, CH_3, J_{CH} = 129
	1.36	3.41, $(CH_3)_2$	31.14	24.12	194.85, *C*Me, J_{WC} = 117[b]
$[(silox)_2W]_2(\mu:\eta^2,\eta^2\text{-}HC_2Ph)(\mu\text{-}H)_2$ (**2c**)	0.96	5.22, J_{WH} = 40, 165			
	0.97	5.27, d, 3, J_{WH} = 39, 184			
	1.40	7.08, Ph			
	1.42	7.67, Ph			
		7.90, Ph			
		11.95, d, CCH, 3			
$[(silox)_2W]_2(\mu\text{-}CH)_2$ (**4a**)	1.20	16.14, J_{WH} = 29[b]	30.74	23.86	303.44, J_{CH} = 165, J_{WC} = 163[b]
$[(silox)_2W]_2(\mu\text{-}CCH_3)_2$ (**4b**)	1.18	5.44, $(CH_3)_2$	31.05	23.26	42.61, CH_3
					319.06, *C*Me, J_{WC} = 160[b]
$[(silox)_2W]_2(\mu\text{-}CH)(\mu\text{-}CPh)$ (**4c**)	1.14	6.93, Ph	31.61	23.55	124.96, *p*-CH
		7.46, Ph			135.09, *m*-CH
		7.73, Ph			159.06, *o*-CH
		16.87, CH, J_{WH} = 28[b]			303.06, μ-CPh
					311.46, μ-CH
$[(silox)_2W]_2(\mu:\eta^2,\eta^2\text{-}MeC_2Me)$ (**8**)	1.10	3.53, $(CH_3)_2$			
	1.35				
$[(silox)_2W]_2(\mu\text{-}CH)(\mu\text{-}CH_2)(H)$ (**9**)[c]	1.04	6.76, dd, J_{HH} = 8, 10,			138.88, ddd, μ-CHH′, J_{CH} = 153,
	1.12	J_{WH} = 105			126, 9, J_{WC} = 97, 50
	1.21	2.55, "t", C*H*H, 11			327.53, d, μ-CH, J_{CH} = 166,
	1.27	10.78, dd, CH*H*, 7, 12			J_{WC} = 152[b]
		21.89, CH, J_{WH} = 18, 26			
$[(silox)_2HTaEt]_2$ (**11**)	1.25	10.66, TaH			
	1.34	2.08, dq, C*H*H, 12, 6			
		2.50, "t", CH_3, 7			
		2.56, dq, CH*H*, 12, 7			
$[(silox)_2TaEt](\mu\text{-}H)_2(\mu\text{-}CHCH_2)$-$[Ta(silox)_2]$ (**12**)	1.09	8.37, br s, TaH	30.80	23.46	20.68, CH_3
	1.29	8.39, br d, TaH, 4	30.98	23.91	53.70, CH_2Me
	1.35	1.54, br m, C*H*HMe, 8	31.03	23.94	72.58, *C*H_2CH
	1.39	2.16, t, CH_3, 8	31.32	24.48	144.27, CH_2*C*H
		2.28, br dq, CH*H*Me, 6, 8			
		3.90, dd, C*H*HCH, 11, 8			
		4.02, dd, CH*H*CH, 12, 8			
		5.02, m, CH_2C*H*, 11			

[a] J_{WH} given if unambiguous. [b] Coupling to two equivalent tungstens according to integrated or estimated intensities (~24.7%). [c] In THF-d_8 at −85 °C; ^{13}C NMR resonances obtained via **9**-$^{13}C_2$.

Table 2. Selected ^{1}H and ^{13}C NMR Data (J in Hz) for Related $W_2(\mu:\eta^2,\eta^2\text{-}C_2H_2)$ and $W_2(\mu\text{-}CH)$ Derivatives

	^{1}H NMR		^{13}C NMR			
compound	δ(C*H*)	J_{WH}	δ(*C*H)	J_{WC}	J_{CH}	ref
$[(silox)_2W]_2(\mu:\eta^2,\eta^2\text{-}C_2H_2)(\mu\text{-}H)_2$ (**2a**)	11.73	0	181.4	115	182	
$W_2(O^tBu)_6(py)(\mu:\eta^2,\eta^2\text{-}C_2H_2)$	5.92	0	120.1	44	184	9
$W_2(OCH_2{}^tBu)_6(py)_2(\mu:\eta^2,\eta^2\text{-}C_2H_2)$	6.51	0	133.2	33, 45	190	15
$W_2(O^iPr)_6(py)_2(\mu:\eta^2,\eta^2\text{-}C_2H_2)$	8.63	0	166.3	42	192	9
$W_2(OSiMe_2{}^tBu)_6(py)(\mu:\eta^2,\eta^2\text{-}C_2H_2)$	6.78	0	145.5	40	189	13
$[(silox)_2W]_2(\mu\text{-}CH)_2$ (**4a**)	16.42	29	303.4	163	165	
$[(silox)_2W]_2(\mu\text{-}CH)(\mu\text{-}O)(\mu\text{-}H)$	19.62	20	319.5	150, 178	168	29
$[Cp^*MeW]_2(\mu\text{-}CH)(\mu\text{-}CMe)$	19.10	16	340.3	142	154	24
$[Cp^*MeW][Cp^*EtW](\mu\text{-}CH)_2$	18.37	16	345.7	145	152	24

spectrum of **4a** is characterized by a single silox peak and a single μ-methylidyne resonance at δ 16.14, with a two-bond tungsten coupling of J_{WH} = 29 Hz whose satellite abundances of 25% indicate a symmetric μ-CH bridge. The methylidyne appears as a doublet at δ 303.44 in the ^{13}C NMR, with a J_{CH} of 165 Hz for the carbon−hydrogen bond, and strong, symmetric coupling to the two tungsten atoms; J_{WC} = 163 Hz. The μ-CH of **4a** is not as deshielded as comparable Cp-based structures (Table 2), but the $W_2(\mu\text{-}CH)_2$ group is easily distinguished from terminal W≡CH ligands (e.g., (^{t}BuO)$_3$W≡CH; δ 252.4, J_{CH} = 150 Hz, J_{WC} = 289 Hz).[9]

Thermolyses of the 2-butyne (**2b**) and phenylacetylene (**2c**) $\mu:\eta^2,\eta^2$-adducts produced the corresponding substituted bis-μ-alkylidynes $[(silox)_2W]_2(\mu\text{-}CMe)_2$ (**4b**) and $[(silox)_2W]_2(\mu\text{-}CH)(\mu\text{-}CPh)$ (**4c**) as yellow and orange crystals, respectively, but more strenuous conditions were required to cleave the C−C bond (~8 h, 120 °C) of these species (eq 2). Equivalent silox and methyl (δ 5.44) groups are observed in the ^{1}H NMR spectrum of **4b**, while an alkylidyne carbon is observed at δ 319.06 in the ^{13}C{^{1}H} NMR spectrum, accompanied by tungsten satellites (J_{WC} = 160 Hz (25%)). The benzylidyne derivative, **4c**, has equivalent silox groups, a μ-CH

Table 3. Crystallographic Data for $[(silox)_2W]_2(\mu\text{-}CCH_3)_2$ (4b) and $[(silox)_2EtTa](\mu\text{-}CHCH_2)(\mu\text{-}H)_2[Ta(silox)_2$ (12)

formula	$W_2Si_4O_4C_{52}H_{114}$	$Ta_2Si_4O_4C_{52}H_{118}$
fw	1283.5	1281.8
space group	*Pbca*	*Pbca*
a (Å)	26.178(11)	26.083(3)
b (Å)	17.083(4)	16.808(2)
c (Å)	28.360(15)	28.764(3)
V (Å^3)	12682(9)	12610(3)
λ (Å)	0.71073 (Mo Kα)	0.71073 (Mo Kα)
μ (mm^{-1})	3.813	3.581
T (K)	298	173(2)
ρ_{calc} (g/cm^3)	1.344	1.350
Z	8	8
R	0.0546[a]	0.0572[a]
R_w	0.0679[b]	0.1307[c]
GOF	0.94[d]	1.117[d]

[a] $R_1 = \sum||F_o| - |F_c||/\sum|F_o|$. [b] $wR_2 = \{\sum[w(F_o - F_c)^2/\sum[wF_o^2]^{1/2}$, where $w^{-1} = \sigma^2F + 0.0026F^2$. [c] $wR_2 = \{\sum[w(F_o^2 - F_c^2)^2/\sum w(F_o^2)^2]^{1/2}$, where $w^{-1} = \sigma^2F$. [d] GOF $= \{\sum w(F_o^2 - F_c^2)^2/(n-p)\}1/2$, n = number of independent reflections, p = number of parameters.

resonance at δ 16.87 (J_{WH} = 28 Hz, 24%) in the ^{1}H NMR spectrum, and alkylidyne carbons resonating at δ 311.46 (μ-CH) and δ 303.06 (μ-CPh) in the $^{13}C\{^1H\}$ NMR spectrum.

With 1 atm H_2 present, the conversion of $[(silox)_2W]_2(\mu\text{:}\eta^2,\eta^2\text{-}C_2Me_2)(\mu\text{-}H)_2$ (**2b**) to $[(silox)_2W]_2(\mu\text{-}CMe)_2$ (**4b**) was severely inhibited, reaching only ~25% conversion after 20 h at 120 °C. Furthermore, when the thermolysis was conducted under 1 atm of D_2 in a sealed NMR tube, loss of the hydride signal and formation of $[(silox)_2W]_2(\mu\text{:}\eta^2,\eta^2\text{-}C_2Me_2)(\mu\text{-}D)_2$ (**2b**-d_2) occurred prior to alkyne cleavage.

3. Structure of $[(silox)_2W]_2(\mu\text{-}CMe)_2$ (4b). A single-crystal X-ray structure (Table 3, Table 4) of $[(silox)_2W]_2(\mu\text{-}CMe)_2$ (**4b**) was obtained, and its molecular and skeletal structures are illustrated in Figure 1. The bis-μ-ethylidene (**4b**) possesses idealized D_2 symmetry and a planar W_2C_2 core that is approximately square, with a W−W single bond distance of 2.720(2) Å and average WCW and CWC angles of 88.5(5)° and 91.5(5)°, respectively. The alkylidyne methyl groups lie in the W_2C_2 plane and occupy large open pockets amidst the silox ligands, but tip slightly toward one side by ~2.6(9)°. As predicted by extended Hückel molecular orbital calculations on related bis-μ-alkylidynes,[25] delocalized bonding is manifested by nearly equivalent W−C distances (1.950(12) Å av).

The periphery of the complex reveals strong steric interactions between the eclipsed silox ligands, which may account for the stretching of the W−W bond, as compared to electronically similar $[(^tBuO)_2W]_2(\mu\text{-}CPh)_2$ (d(W−W) = 2.665(1) Å; ∠C−W−C = 93.1°);[6] the C−W−C angles in **4b** are correspondingly more acute. Inter-

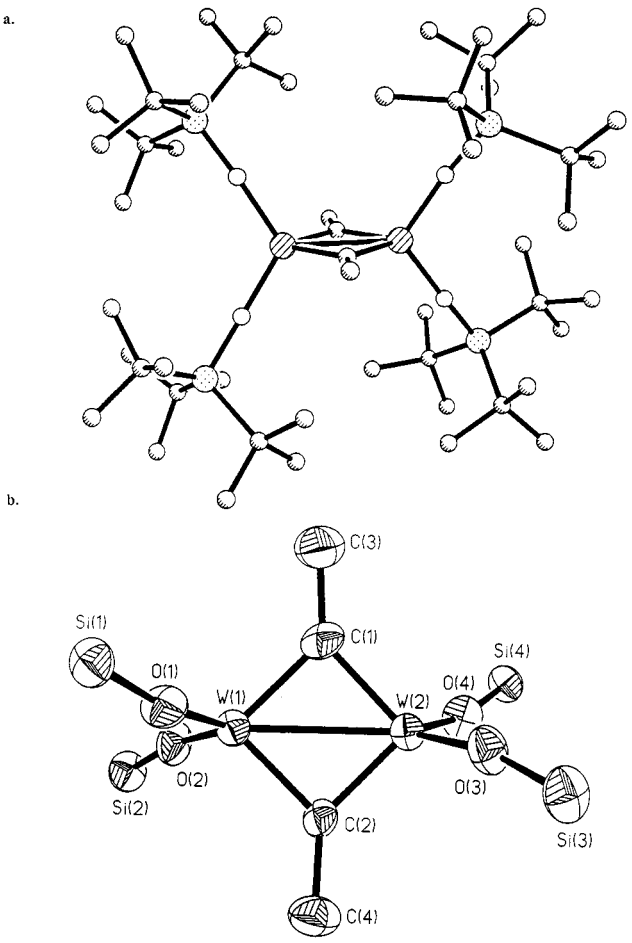

Figure 1. Molecular structure of $[(silox)_2W]_2(\mu\text{-}CMe)_2$ (**4b**): (a) view along the alkylidyne vector, emphasizing the steric interactions among the silox ligands; (b) inner coordination sphere.

nuclear steric repulsions may also contribute to the rather small O−W−O angles of 114.7(35)°, but a more dramatic result of the steric crowding is the twisting of the O−W−O planes away from their ideal eclipsed geometry, resulting in a dihedral angle of ~10°. Despite these core distortions, the silox ligands have normal bond lengths ($W-O_{av}$ = 1.895(8) Å) and angles ($W-O-Si_{av}$ = 167.8(6)°). The interlocking of the silox *tert*-butyl groups may account for the low, room-temperature solubility of **4a**−**c**. Assuming the solution structure of $[(silox)_2W]_2(\mu\text{-}CH)(\mu\text{-}CPh)$ (**4c**) resembles that of **4b**, its likely C_2 symmetry is contradicted by the observation of a single silox resonance. Access to an eclipsed conformation or transition state is energetically feasible; hence a fluxional process between diasterotopic silox groups in the μ-alkylidynes **4a**−**c** is likely. A related

Table 4. Selected Interatomic Distances (Å) and Angles (deg) for $[(silox)_2W]_2(\mu\text{-}CCH_3)_2$ (4b)

W1−W2	2.720(2)	W1−C1	1.954(12)	W1−C2	1.945(11)
W2−C1	1.959(12)	W2−C2	1.940(11)	C1−C3	1.470(18)
C2−C4	1.523(18)	W1−O1	1.902(8)	W2−O2	1.906(8)
W2−O3	1.895(8)	W2−O4	1.876(7)	Si1−O1	1.663(9)
Si2−O2	1.660(9)	Si2−O3	1.661(9)	Si4−O4	1.680(8)
W1−C1−W2	88.1(5)	W1−C2−W2	88.9(5)	C1−W1−C2	91.5(5)
C1−W2−C2	91.5(5)	W1−C1−C3	133.6(10)	W2−C1−C3	138.4(10)
W1−C2−C4	133.0(8)	W2−C2−C4	138.1(9)	W2−W1−O1	120.4(2)
W2−W1−O2	122.6(2)	W1−W2−O3	124.0(2)	W1−W2−O4	123.9(2)
O1−W1−O2	117.1(3)	O3−W2−O4	112.2(3)	W1−O1−Si1	168.0(5)
W1−O2−Si2	169.8(5)	W2−O3−Si3	166.6(6)	W2−O4−Si4	166.7(6)

interchange is apparently responsible for silox signal averaging in ^{1}H NMR spectra of $[(silox)_2W]_2(\mu\text{-CH})(\mu\text{-O})(\mu\text{-H})$.[29]

The low solubility of **4a**−**c** in comparison to **2a**−**c** correlates with the restricted motion of their silox ^{t}Bu groups, which suggests steric destabilization in accord with the structural study above. Despite apparently severe steric interactions, no reversibility was observed when **4a** and **4b** were exposed to 3 atm H_2, even at high temperatures (>100 °C) and extended reaction times (>1 day). These C−C bond cleavage reactions are favorable due to the formation of the bis-μ-alkylidyne core, which is a proven thermodynamic "sink" in diverse tungsten systems.[19−28]

4. μ-Ethylidyne from $[(silox)_2W(CH_2CH_3)]_2$ (5). The thermodynamic driving force associated with bis-μ-alkylidyne formation is further evidenced by the appearance of $[(silox)_2W]_2(\mu\text{-CMe})_2$ (**4b**) as a product of a seemingly unrelated reaction, the thermal degradation of $[(silox)_2W(CH_2CH_3)]_2$ (**5**, eq 3).[30] When **5** is heated to

$$\underset{\mathbf{5}}{[(silox)_2W(CH_2CH_3)]_2} \xrightarrow[30\ min]{100\ °C} 1/2\ \underset{\mathbf{4b}}{[(silox)_2W]_2(\mu\text{-CMe})_2} + 1/2\ \underset{\mathbf{1}}{[(silox)_2WH]_2} + EtH \quad (3)$$

100 °C for 30 min in the presence of an additional 2 equiv of ethylene, **4b** is quantitatively generated along with 2 equiv of C_2H_6 (eq 4). If additional ethylene is not

$$\mathbf{5} + 2\ C_2H_4 \xrightarrow[30\ min]{100\ °C} \mathbf{4b} + 2\ EtH \quad (4)$$

present, the products are a 1:1:2 mixture of **4b**, $[(silox)_2WH]_2$ (**1**), and ethane. Formation of **4b** is considered to be promoted by ethylene released upon successive β-H-elimination reactions of the diethyl dinuclear **5** that afford dihydride **1**, a pathway previously established.[30] The reversibility of the β-H-elimination process was also presumed to be responsible for the inability to selectively label **5** via **1** and C_2D_4 or **1**-d_2 and C_2H_4; rapid total label scrambling was noted.

5. 2-Butyne Trapping of Putative $[(silox)_2W]_2$. The conversion of the μ-alkyne dihydrides **2a**−**c** to bis-μ-alkylidynes **4a**−**c** prompted consideration of $[(silox)_2W]_2(\mu{:}\eta^2,\eta^2\text{-}RC_2R')$ as an intermediate. Previous studies[30,35,36] suggested that the putative quadruple-bonded complex $[(silox)_2W]_2$ (**7**) could be trapped by added ligands; hence $(silox)_2ClW{\equiv}WCl(silox)_2$ (**3**) was reduced with a >200-fold excess of 2-butyne present according to eq 5. An assay of the products revealed a

$$\underset{\mathbf{3}}{[(silox)_2WCl]_2} + MeC{\equiv}CMe \xrightarrow[25\ °C,\ 1.5\ h,\ -2\ NaCl]{Na/Hg,\ DME} \underset{\mathbf{6}}{(silox)_2HW{\equiv}W(OSi^tBu_2CMe_2CH_2)(silox)} + \underset{\mathbf{8}}{[(silox)_2W]_2(\mu{:}\eta^2,\eta^2\text{-}MeC_2Me)} \quad (5)$$

~3:7 ratio of the cyclometalated triple-bonded complex $(silox)_2HW{\equiv}W(OSi^tBu_2CMe_2CH_2)(silox)$ (**6**)[30] and another species with a singlet at δ 3.53 in addition to diastereotopic silox groups, tentatively formulated as $[(silox)_2W]_2(\mu{:}\eta^2,\eta^2\text{-}MeC_2Me)$ (**8**). Addition of 1 atm of H_2 (or D_2) to the crude mixture containing **8** afforded $[(silox)_2W]_2(\mu{:}\eta^2,\eta^2\text{-}MeCCMe)(\mu\text{-H})_2$ (**2b**, eq 6) (or **2b**-d_2) and **1** (or **1**-d_2), presumably derived from **6**.[30]

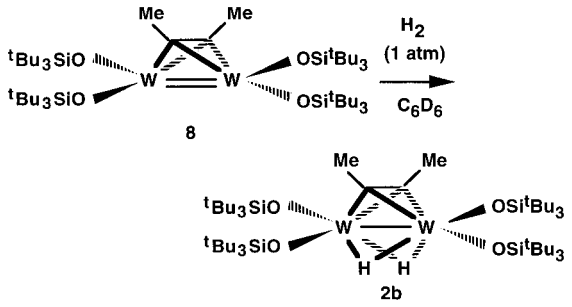

(6)

Similarly, thermolysis (80 °C, 5 h) of the mixture converted **8** to $[(silox)_2W]_2(\mu\text{-CMe})_2$ (**4b**), and the relative concentration of cyclometalated product **6** remained constant.

$$\mathbf{8} \xrightarrow[C_6D_6]{5\ h,\ 80\ °C} \underset{\mathbf{4b}}{[(silox)_2W]_2(\mu\text{-CMe})_2} \quad (7)$$

6. Ethylene Dehydrogenation and Cleavage by Putative $[(silox)_2W]_2$. Given the success of 2-butyne trapping of the reduction product(s) of $[(silox)_2WCl]_2$ (**3**), scavenging with ethylene was attempted. Na/Hg reduction of $[(silox)_2WCl]_2$ (**3**) in DME under 1 atm C_2H_4 at 25 °C produced a red solution within 5 min. Dissipation of the color over 15−20 min occurred concurrently with the precipitation of a yellow solid, $[(silox)_2W]_2(\mu\text{-CH})_2$ (**4a**), which was isolated in 68% yield from hexanes (eq 8). Toepler analysis of the volatiles revealed the evolu-

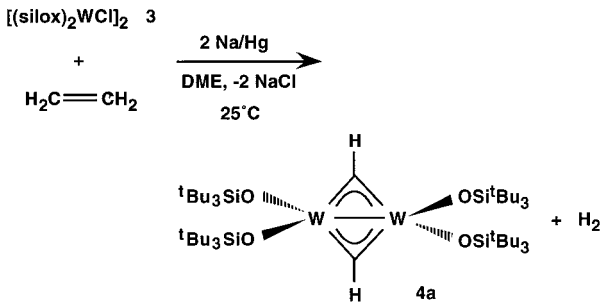

(8)

tion of 0.79 equiv of H_2 as a byproduct of the reaction. The generation of H_2 is further corroborated by the formation of $[(silox)_2WH]_2$ (**1**) as a spurious product (10−20% yield) when the reduction is carried out under low (300 Torr) pressures of ethylene. The reduced intermediate—presumably $[(silox)_2W]_2$ (**7**)—is competitively scavenged by the H_2 evolved from the dehydrogenation of ethylene.

The AA′XX′ spin system of the $W_2(\mu\text{-CH})_2$ core (J_{HH} = 9, $^1J_{CH}$ = 165, $^3J_{CH}$ = 3, $J_{CC} \approx 0$ Hz)[37] was evident in the NMR spectra of a sample of **4a**-$^{13}C_2$ prepared by reduction of **3** under $^{13}C_2H_4$. A crossover experiment,

(35) Miller, R. L. Ph.D. Thesis, Cornell University, 1993.
(36) Mayol, A.-R. Ph.D. Thesis, Cornell University, 1999.
(37) Leydon, D. E.; Cox, R. H. *Analytical Applications of NMR*; John Wiley & Sons: New York, 1977.

in which a mixture of C_2H_4 and $^{13}C_2H_4$ was admitted to the reaction vessel, showed only **4a** and **4a**-$^{13}C_2$ as products, confirming that the conversion proceeds without the involvement of monomeric intermediates or other ethylene-scrambling pathways. Cyclometalated (silox)$_2$HW≡W(OSi^{t}Bu$_2$CMe$_2$CH$_2$)(silox) (**6**) was ruled out as the source of reactivity, since it is unreactive toward C_2H_4 and other substrates (2-butyne, CO, etc.).

The red intermediate persisted in solution for >3 h at −78 °C and was monitored by low-temperature NMR spectroscopy. Solutions of [(silox)$_2$WCl]$_2$ (**3**) in THF-d_8 were reduced under C_2H_4 and $^{13}C_2H_4$ for ^{1}H and ^{13}C NMR spectral analysis, respectively. Upon development of the red color, each solution was cooled to −78 °C, degassed to remove excess ethylene, and decanted into an NMR tube that was sealed for monitoring. The conversion to [(silox)$_2$W]$_2$(μ-CH)$_2$ (**4a**) from the red intermediate was clean in the absence of additional C_2H_4 or reducing agent, confirming that reduction and ethylene uptake are complete at that stage.

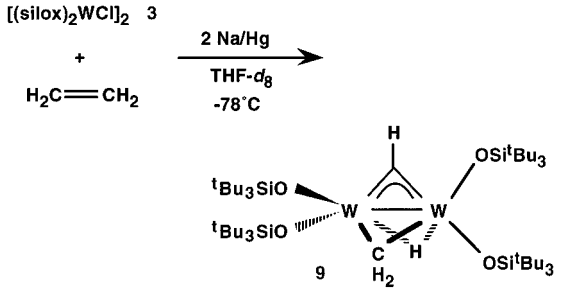

(9)

At −85 °C, four proton signals were assigned to ethylene-derived ligands, and four silox groups were observed, corresponding to the intermediate [(silox)$_2$W]$_2$(μ-CH)(μ-CH$_2$)(H) (**9**) shown in eq 9. In the ^{1}H NMR spectrum, a μ-methylidyne singlet at δ 21.89 displayed couplings to ^{183}W of ∼18 and 26 Hz, and in the ^{13}C NMR spectrum, the μ-methylidyne carbon was identified at δ 327.53 (J_{CH} = 166 Hz; $J_{WC} \approx J_{W'C}$ = 152 Hz, 24%); no carbon−carbon coupling was discerned for **9**-$^{13}C_2$. A hydride ligand at δ 6.76 had tungsten satellites suggestive of bridging coordination (J_{WH} = 105 Hz), but the assignment is ambiguous because the intensities did not reliably integrate for two tungstens. The hydride was coupled to inequivalent methylene protons (dd, J_{HH} = 8, 10 Hz), and a weak coupling to the methylene carbon was evident from the broadening and loss of definition in the hydride multiplet in **9**-$^{13}C_2$.

A methylene carbon resonating at δ 138.88 in the ^{13}C NMR spectrum was found to bridge the W centers (J_{WC} = 50, 97 Hz), and at −85 °C it showed coupling to two disparate protons: one was found at δ 2.55 ("t", J_{HH} = 11 Hz) in the ^{1}H NMR spectrum with J_{CH} = 126 Hz and the other at δ 10.78 (dd, J_{HH} = 7, 12) with a larger coupling constant of J_{CH} = 150 Hz. As the sample temperature was raised, the two methylene proton signals exchange-broadened and coalesced at ca. 5 °C, via a process whose $\Delta G^{\ddagger}$ = 11(1) kcal/mol. The ^{13}C signal at δ 138.88 simultaneously merged to a sharp triplet with J_{CH} = 137 Hz. Indications of silox resonance coalescence or hydride participation, etc., are absent; consequently, the simplest path to exchange of the methylene protons involves a μ-CH$_2$ to η^1-CH$_2$ conversion, methylene rotation, and reconnection within a framework effectively locked by the typical, pseudo-D_{2d} arrangement of the siloxides. Note that the isoelectronic μ-oxo derivative [(silox)$_2$W]$_2$(μ-CH)(μ-O)(H) exhibited coalescence of its four silox resonances at 80 °C ($\Delta G^{\ddagger}$ = 17 (1) kcal/mol);[29] hence interchange of silox ligands is probably difficult due to steric interactions.

7. μ-Vinyl Formation from [(silox)$_2$TaH$_2$]$_2$ and Ethylene. Given the propensity of [(silox)$_2$W(CH$_2$CH$_3$)]$_2$ (**5**) to form the bis-μ-ethylidyne [(silox)$_2$W]$_2$(μ-CMe)$_2$ (**4b**) and the unusual carbon−hydrogen and carbon−carbon bond scission of ethylene by putative [(silox)$_2$W]$_2$ (**7**), the reactivity of ethylene with [(silox)$_2$TaH$_2$]$_2$ (**10**)[38] was explored in order to seek related chemistry. Treatment of **10** with excess C_2H_4 in C_6D_6 incurred the immediate formation of [(silox)$_2$HTaEt]$_2$ (**11**, eq 10), whose probable C_2 symmetry was signified by diastereotopic methylene protons at δ 2.08 (dq, J_{HH} = 12, 6) and δ 2.56 (dq, J_{HH} = 12, 7) in addition to inequivalent silox resonances.

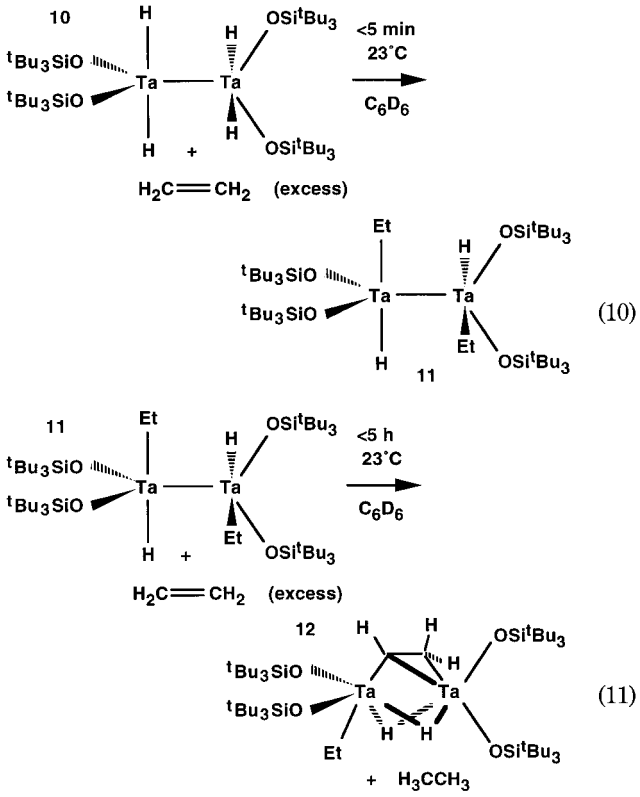

(10)

(11)

Although **11** can be identified by ^{1}H NMR spectroscopy, with excess ethylene conversion to the final product, orange [(silox)$_2$EtTa](μ-CHCH$_2$)(μ-H)$_2$[Ta(silox)$_2$] (**12**), is swift and complete at 23 °C within 5 h and ethane is a byproduct. In the ^{1}H NMR spectrum, four inequivalent silox resonances are observed and two broad hydride resonances appear at d 8.37 and δ 8.39, with the latter exhibiting coupling (4 Hz) tentatively assigned to one of the diasterotopic CH*H*Me protons (δ 1.54, 2.28; J = 8), whose resonances are also broadened. The IR spectrum of **12** manifests a broad hydride absorption at 1603 cm^{-1} that is assigned to bridging hydrides. Since this frequency is on the high end for Ta$_2$(μ-H) derivatives,[38] asymmetric bridges are tentatively suggested. The vinyl

(38) Miller, R. L.; Toreki, R.; LaPointe, R. E.; Wolczanski, P. T.; Van Duyne, G. D.; Roe, D. C. *J. Am. Chem. Soc.* **1993**, *115*, 5570−5588.

Table 5. Selected Interatomic Distances (Å) and Angles (deg) for [(silox)$_2$EtTa](μ-CHCH$_2$)(μ-H)$_2$[Ta(silox)$_2$] (12)

Ta1−Ta2	2.9991(6)	Ta1−C1	2.302(18)	C3−C4	1.33(2)
Ta1−O1	1.874(7)	Ta1−C2	2.218(16)	Si1−O1	1.680(7)
Ta1−O2	1.880(7)	Ta2−C1	2.096(18)	Si2−O2	1.673(7)
Ta2−O3	1.895(7)	Ta2−C3	2.191(14)	Si3−O3	1.651(7)
Ta2−O4	1.887(7)	C1−C2	1.62(2)	Si4−O4	1.672(7)
Si−C$_{av}$	1.918(20)	C−C$_{av}$	1.546(32)		
O1−Ta1−O2	110.1(3)	O3−Ta2−C3	97.0(6)	Ta1−C2−C1	71.8(9)
O1−Ta1−C2	101.3(4)	O4−Ta2−C1	111.0(5)	Ta1−O1−Si1	173.9(5)
O1−Ta1−C1	106.8(5)	O4−Ta2−C3	101.3(4)	Ta1−O2−Si2	175.7(4)
O2−Ta1−C2	104.2(5)	C1−Ta2−C3	136.8(6)	Ta2−O3−Si3	171.2(5)
O2−Ta1−C1	134.5(5)	Ta1−C1−Ta2	85.9(7)	Ta2−O4−Si4	173.9(5)
C1−Ta1−C2	41.9(6)	Ta2−C1−C2	137.8(12)	O−Si−C$_{av}$	106.5(10)
O3−Ta2−O4	111.1(3)	Ta2−C3−C4	127(2)	C−Si−C$_{av}$	112.3(12)
O3−Ta2−C1	97.3(5)	Ta1−C1−C2	66.3(8)	Si−C−C$_{av}$	111.1(21)
				C−C−C$_{av}$	107.7(17)

is observed by coupled ^{1}H NMR spectroscopic resonances at δ 3.90, 4.02, and 5.02 and ^{13}C{^{1}H} NMR resonances at δ 72.58 (CH$_2$) and δ 144.27 (CH).

A third equivalent of ethylene is needed for the transformation from **11** to **12**, since ethane is formed. Without ethylene, **11** slowly disproportionates to **10** and **12** (∼1:2), and with only one additional equivalent, **11** was converted to **12** over the course of 4 days. Rough rate measurements conducted with 10−75 equiv (2−19 solution equiv) revealed an order in [C_2H_4] that was significantly less than 1 (0.1−0.2). Unfortunately, the mechanstic details of the **11** to **12** conversion have been difficult to determine, because the addition of C_2D_4 to **10** or the combination of C_2H_4 and **10**-d_4 resulted in rapid label scrambling—presumably via β-H-elimination/insertion paths—throughout the ethyl groups of **11** and in all positions of **12**. When treated with excess C_2D_4, **12** exhibited a minor amount (<10%) of H/D exchange in its hydride and ethyl positions within 40 h. Less than 50% exchange in these positions was evident after 9 days, and after 60 days additional H/D exchange into the vinyl positions was observed. A rate comparison between **10** and C_2H_4 (4 equiv) versus **10**-d_4 and C_2D_4 (4 equiv) provided a phenomenological k_H/k_D for the **11**/**11**-d_{10} to **12**/**12**-d_{10} conversions of 9(1).

8. Structure of [(silox)$_2$EtTa](μ-CHCH$_2$)(μ-H)$_2$[Ta(silox)$_2$] (12). An X-ray crystal structure (Table 3, Table 5) of [(silox)$_2$EtTa](μ-CHCH$_2$)(μ-H)$_2$[Ta(silox)$_2$] (**12**) confirmed the configuration based on NMR spectroscopy. Figure 2. reveals a D_2 arrangement of (silox)$_2$-Ta cores connected by the bridging vinyl group. Although the structure clearly supports the spectral data, some geometric parameters of the bridge are imprecise (e.g., d(C1−C2) = 1.62(2) Å, ∠Ta2−C1−C2 = 137.8-(12)°), as is often the case for relatively light atoms positioned between two heavy atoms. The pseudo-sp^2 vinyl tantalum−carbon bond (d(Ta2−C1) = 2.096(18) Å) is shorter than that of its sp^3 ethyl counterpart (d(Ta2−C3) = 2.191(14) Å), and both are shorter than the "tantalum−olefin" distances (d(Ta1−C1) = 2.302-(18) Å, d(Ta1−C2) = 2.218(16) Å). The ∠Ta2−C3−C4 = 127(2)° angle may indicate a modest agostic interaction, but it is also consistent with the steric demands of the Ta2 core.

The hydrides could not be detected with confidence and have been placed in bridging positions commensurate with the methine bridging angle of ∠Ta1−C1−Ta2 = 85.9(7)° (d(Ta−Ta) = 2.9996(6) Å, ∠Ta1−C1−C2 = 66.3(8)°) and the geometries of each tantalum's core. The intersilox angle ∠O3−Ta2−O4 = 111.1(3)° and remaining core angles (i.e., ∠C1−Ta2−O3 = 97.3(5)°, ∠C1−Ta2−O4 = 111.0(5)°, ∠C3−Ta2−O3 = 97.0(6)°, ∠C3−Ta2−O4 = 101.3 (4)°) reveal a splay of the ligands (∠C1−Ta2−C3 = 136.8(6)°) that can accommodate a pair of bridging hydrides in the O4−Ta2−O3 plane essentially opposite O4. Likewise, the O1−Ta1−O1 angle of 110.1(3)° and the other Ta1 core angles (i.e., ∠C1−Ta1−O1 = 106.8(5)°, ∠C1−Ta1−O2 = 134.5(5)°, C2−Ta1−O1 = 101.3(4)°, C2−Ta1−O2 = 104.2(5)°) leave a related pocket for the μ-H ligands above the C1−O1−O2 plane opposite C2.

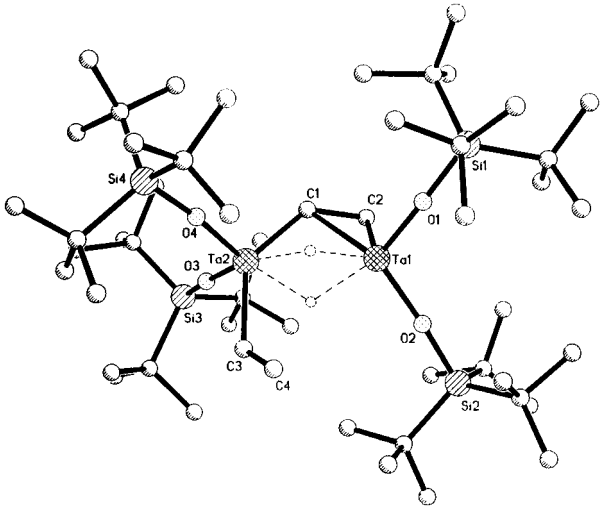

Figure 2. Molecular structure of [(silox)$_2$TaEt](μ-H)$_2$(μ-CHCH$_2$)[Ta(silox)$_2$] (**12**). The hydrides were not located and have been placed in appropriate bridging positions.

Discussion

Structures and Spectroscopy. Interligand repulsions within the tetrasilox dimetal cores dominate the structural features manifested by the spectroscopy and diffraction studies. In the thermally unstable μ:η^2,η^2-acetylene adducts, [(silox)$_2$W]$_2$(μ:η^2,η^2-RCCR′)(μ-H)$_2$ (R = R′ = H, **2a**; CH$_3$, **2b**; R = H, R′ = Ph, **2c**), a plausible symmetric C_{2v} environment would dictate equivalent silox groups, yet a distortion to C_2 renders the hydrides asymmetric and two different silox ligands for **2a** and **2b**; the phenylacetylene derivatives exhibit two inequivalent hydrides and four different silox groups. Symmetrical bridging hydrides were tentatively pro-

Scheme 1

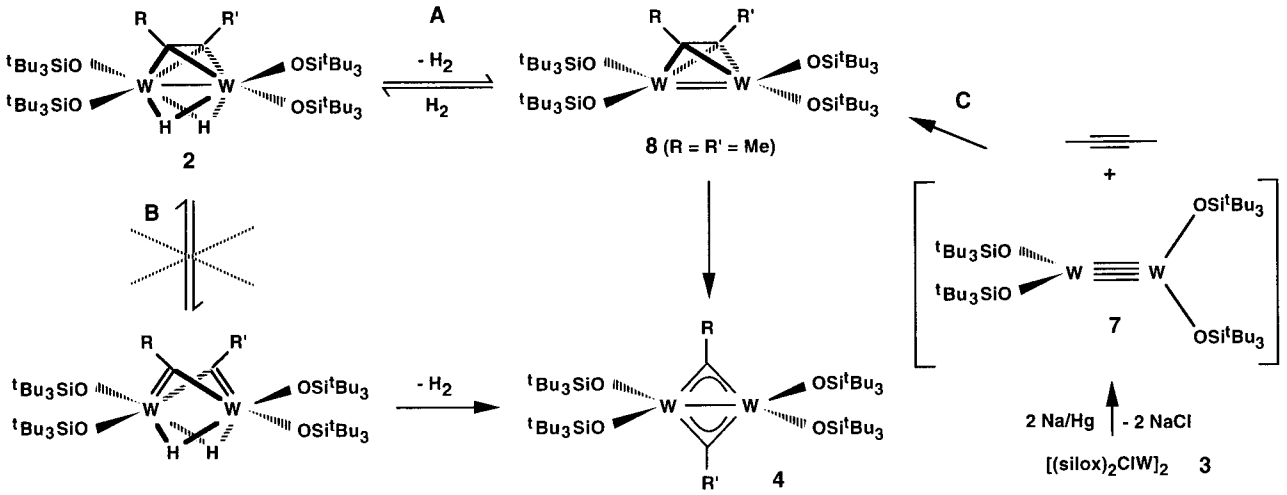

posed for the related tetrahydride, D_{2d} $[(silox)_2W]_2(\mu\text{-}H)_4$,[30] and a symmetrical acetylene and hydride environment for **2a** and **2b** would be expected were it not for the eclipsing of the siloxides in C_{2v}. In the solid state structure of $[(silox)_2W]_2(\mu\text{-}CMe)_2$ (**4b**), a subtle rotation of a $[(silox)_2W]$ unit by 10° lowers the symmetry from D_{2h} to D_2, and it is likely that the same sterically derived distortion is responsible for the lower symmetries of **2a**, **2b**, and **2c**. It is difficult to know whether the hydrides would be symmetrically bridged in the absence of the silox steric constraints, but it is notable that the average J_{WH} in **2a**, **2b**, and **2c** is similar to that of $[(silox)_2W]_2(\mu\text{-}H)_4$, as previously stated.

Mechanistic Evaluations. 1. Alkyne Scission. While the initial alkyne adducts $[(silox)_2W]_2(\mu{:}\eta^2,\eta^2\text{-}RCCR')(\mu\text{-}H)_2$ (R = R′ = H, **2a**; CH_3, **2b**; R = H, R′ = Ph, **2c**) appear to be structurally related to numerous others,[9−21] further reactions with RCCR′ to form C_4-containing products[15−21] or direct cleavages[2−6,9] to $(silox)_2(H)W{\equiv}CR/R'$ or $(silox)_2W{=}CHR/R'$[39,40] species were not observed. Instead, cleavage occurs with reductive elimination of H_2. One ostensibly analogous reaction is the high-temperature reaction of $(^tBuO)_6W_2$ with diphenylacetylene, which proceeds with apparent decomposition or transfer of two $^tBuO^\bullet$ groups to form a product mixture including a bis-μ-alkylidyne, $[(^tBuO)_2W]_2(\mu\text{-}CPh)_2$.[6] No intermediates were detected, and it was surmised that alkoxide loss *preceded* alkyne binding. It is also notable that another siloxide-based alkyne adduct, $(^tBuMe_2SiO)_6W_2(\mu{:}\eta^2\text{-}C_2H_2)(py)$, does not promote C−C cleavage but instead eliminates $^tBuMe_2SiOH$ in hydrocarbon solutions, forming a μ-ethynyl complex, $(^tBuMe_2SiO)_5W_2(\mu{:}\eta^2\text{-}CCH)(py)$.[13]

Two mechanisms for the dehydrogenation and alkyne scission of $[(silox)_2W]_2(\mu{:}\eta^2,\eta^2\text{-}RCCR')(\mu\text{-}H)_2$ (R = R′ = H, **2a**; CH_3, **2b**; R = H, R′ = Ph, **2c**) to give $[(silox)_2W]_2(\mu\text{-}CR)(\mu\text{-}CR')$ (R = R′ = H, **4a**; CH_3, **4b**; R = H, R′ = Ph, **4c**) are presented in Scheme 1. In **A**, reversible dihydrogen elimination is followed by C−C bond cleavage of a $[(silox)_2W]_2(\mu{:}\eta^2,\eta^2\text{-}RCCR')$ (**8** if R = R′ = Me) intermediate; alternatively, alkyne cracking may occur first (**B**) followed by dehydrogenation. In **B**, the initial C−C cleavage step is analogous to a microscopic step in the alkyne scission reactions promoted by $W_2(^tBuO)_6$.[2−6,9] Justification for dihydrogen elimination is provided by observation of Cl_2, Br_2, and ROOR oxidative additions to the W−W bond in bis-μ-alkylidynes,[26,27] reactions that constitute the microscopic reverse.

Recall that D_2 was observed to wash into the hydride positions of **2b** when 1 atm D_2 was present, forming **2b**-d_2 prior to conversion to **4b**. While associative H_2/D_2 exchange cannot be ruled out (HD was not observed), it is likely that reversible addition of dihydrogen, as in path **A**, permits $[(silox)_2W]_2(\mu{:}\eta^2,\eta^2\text{-}RCCR')$ to form and cleavage occurs via this intermediate. H_2/D_2 exchange may not rule out **B**, but inhibition of cleavage by the presence of excess dihydrogen (or D_2) and the independent entry (**C**) to $[(silox)_2W]_2(\mu{:}\eta^2,\eta^2\text{-}MeCCMe)$ (**8**) via 2-butyne trapping of putative $[(silox)_2W]_2$ (**7**, eq 5) strongly support **A**. The cleavage of **8** to **4b** occurs under conditions milder than those of **2b** to **4b**, consistent with the dihydrogen preequilibrium evident in the latter path. Path **B** would show H_2 inhibition and H_2/D_2 exchange only if the dihydrogen loss step is reversible, but none of the bis-μ-alkylidynes (i.e., **4a**, **4b**, nor **4c**) could be hydrogenated back to **2a**, **2b**, or **2c**.

2. Ethylene Scission. The generation of $[(silox)_2W]_2(\mu\text{-}CH)_2$ (**4a**) upon reduction of $(silox)_2ClW{\equiv}WCl(silox)_2$ (**3**) in the presence of C_2H_4 represents a formal dehydrogenation and C−C cleavage of ethylene, a reaction unprecedented in tungsten chemistry. A plausible scenario for ethylene cleavage is indicated in Scheme 2. In it, the putative quadruply bonded intermediate, $[(silox)_2W]$ (**7**), is invoked as the C−H bond activating species. Dichloride **3** did not interact with any olefin, ethylene or alkyne, even at high temperatures (>100 °C). Cyclometalation product $(silox)_2HW{\equiv}W(OSi^tBu_2CMe_2CH_2)(silox)$ (**6**) can also be eliminated as the source of reactivity since it responded only sluggishly to ethylene in NMR tube reactions. Some product of the reduction of **3** must therefore be responsible for the activation of C_2H_4, given the mild conditions (≤25 °C), and a low coordinate transient such as **7** has tremen-

(39) Holmes, S. J.; Clark, D. N.; Turner, H. W.; Schrock, R. R. *J. Am. Chem. Soc.* **1982**, *104*, 6322−6329.
(40) Chacon, S. T.; Chisholm, M. H.; Eisenstein, O.; Huffman, J. C. *J. Am. Chem. Soc.* **1992**, *109*, 8497−8509.

Scheme 2

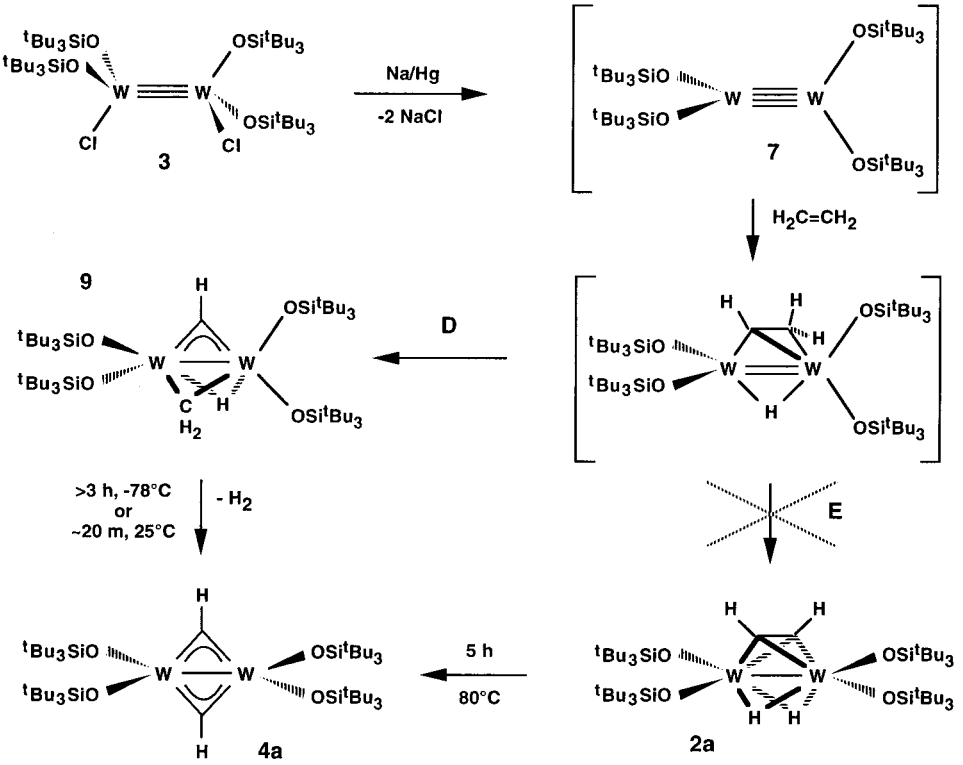

dous appeal on the basis of the favorable sterics and electronics of its D_{2d} structure.[30]

Oxidative addition of a ethylene carbon−hydrogen bond across the W≡W bond of putative $[(silox)_2W]_2$ (**7**) leads to a μ-vinyl hydride. A similar vinylic C−H activation by a metal−metal multiple bond is implicated when $(Cp^*Ta)_2(\mu\text{-}X)_4$ (X = Cl, Br) reacts with ethylene to form a $Ta_2(\mu{:}\eta^1,\eta^2\text{-}CHCH_2)(\mu\text{-}H)$ complex.[41,42] Furthermore, generation of $[(silox)_2EtTa](\mu\text{-}CHCH_2)(\mu\text{-}H)_2[Ta(silox)_2]$ (**12**) via $[(silox)_2HTaEt]_2$ (**11**) upon exposure of $[(silox)_2TaH_2]_2$ (**10**) to C_2H_4 lends credence to such an intermediate in a tetrasiloxdimetallic system. An α- or β-H elimination from the μ-vinyl ligand should lead to $[(silox)_2W]_2(\mu{:}\eta^2,\eta^2\text{-}HCCH)(\mu\text{-}H)_2$ (**2a**) as path **E** indicates, but the conditions for ethylene cleavage are markedly milder than those for the thermal μ-alkyne scission of **2a**; mechanism **E** is therefore discounted. Furthermore, exposure of **2a** to C_2H_4 and THF did not induce formation of **4a**, thereby supporting exclusion of the **E** pathway.

Cleavage of the carbon−carbon bond in the proposed $[(silox)_2W]_2(\mu{:}\eta^1,\eta^2\text{-}CHCH_2)(\mu\text{-}H)$ transient would generate the observed intermediate $[(silox)_2W]_2(\mu\text{-}CH)(\mu\text{-}CH_2)(H)$ (**9**). The microscopic reverse of this reaction has been inferred in the oxidatively induced coupling of μ-methylene and μ-methylidyne ligands in a dirhodium complex; because of subsequent reactivity, the μ-vinyl product was not observed, but its intermediacy was implied by a series of labeling experiments.[43] Note that the asymmetry of the μ-methylene group in **9** may play a role in allowing a low kinetic barrier for the 1,2-H_2-elimination to form $[(silox)_2W]_2(\mu\text{-}CH)_2$ (**4a**).[17,18,44−48]

3. μ-Ethylidene Formation. Since the thermal conversion of $[(silox)_2W(CH_2CH_3)]_2$ (**5**) to $[(silox)_2W]_2(\mu\text{-}CMe)_2$ (**4b**) proceeds cleanly, even under conditions of low ethylene concentration, any steps occurring before uptake of the first C_2H_4 molecule may be reversible. In addition, treatment of **5** with C_2D_4 revealed H/D scrambling into all ethyl groups and the added ethylene, consistent with rapid and reversible β-H/D-eliminations prior to conversion to **5**. As a consequence, mechanistic information for the **5** → **4b** transformation is extremely limited.

Ignoring stereochemical aspects of the mechanism, Scheme 3 illustrates a plausible sequence featuring oxidative addition of an α-methylene unit across the metal−metal bond and hydrogen migration as the initial step. Ethylene insertion into the hydride affords the means to conduct an α-abstraction[17,18,44−48] that generates the first μ-CH bridge and ethane. A repeat of this sequence involving a hydrogenation of a second equivalent of C_2H_4 provides a pathway to **5** as the second μ-methine is formed. Scheme 3 accounts for the uptake of 2 equiv of free ethylene and the failure to observe quantitative conversion in its absence.

(41) Ting, C.; Messerle, L. *J. Am. Chem. Soc.* **1987**, *109*, 6506−6508.
(42) For a reversible CH activation in related metal−metal bonded systems, see: Chisholm, M. H.; Huang, J. H.; Huffman, J. C.; Parkin, I. P. *Inorg. Chem.* **1997**, *36*, 1642−1651.
(43) Maitlis, P. M.; Saez, I. M.; Meanwell, N. J.; Isobe, K.; Nutton, A.; de Miguel, A. V.; Bruce, D. W.; Okeya, S.; Bailey, P. M.; Andrews, D. G.; Ashton, P. R.; Johnstone, I. R. *New J. Chem.* **1989**, *13*, 419−425.
(44) Schrock, R. R.; Seidel, S. W.; Mösch-Zanetti, N. C.; Shih, K.-Y.; O'Donohue, M. B.; Davis, W. M.; Reiff, W. M. *J. Am. Chem. Soc.* **1997**, *119*, 11876−11893
(45) Schrock, R. R.; Seidel, S. W.; Mösch-Zanetti, N. C.; Dobbs, D. A.; Shih, K.-Y.; Davis, W. M. *Organometallics* **1997**, *16*, 5195−5208.
(46) Davies, D. L.; Gracey, B. P.; Guerchais, V.; Knox, S. A. R.; Orpen, A. G. *J. Chem. Soc., Chem. Commun.* **1984**, 841−843.
(47) Connelly, N. G.; Forrow, N. J.; Gracey, B. P.; Knox, S. A. R.; Orpen, A. G. *J. Chem. Soc., Chem. Commun.* **1985**, 14−16.
(48) Blau, R. J.; Chisholm, M. H.; Eichhorn, B. W.; Huffman, J. C.; Kramer, K. S.; Lobkovsky, E. B.; Streib, W. E. *Organometallics* **1995**, *14*, 1855−1869.

Scheme 3

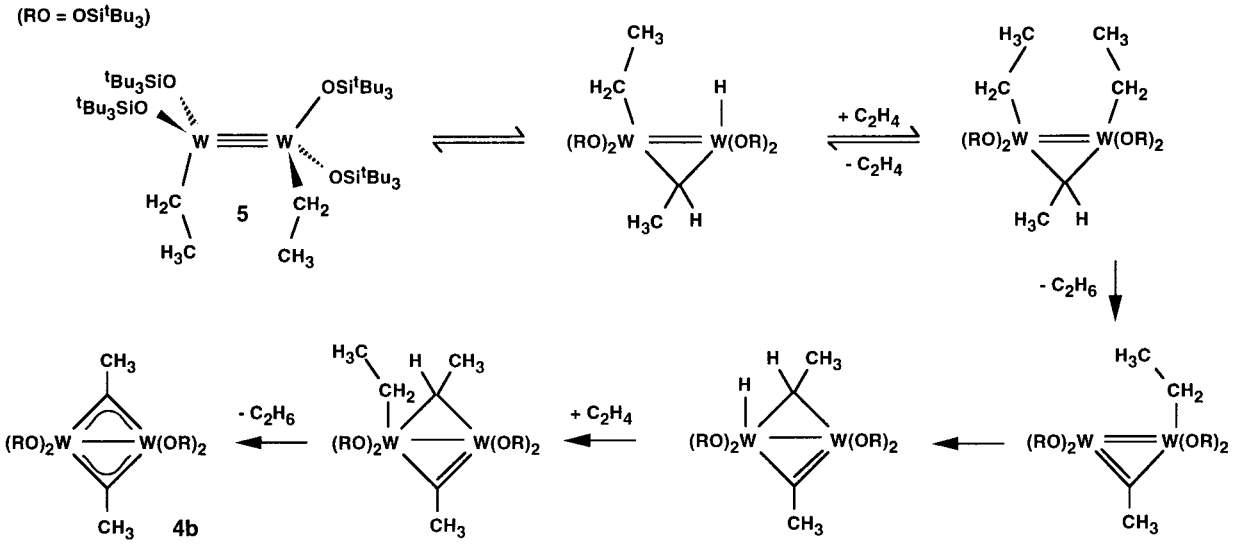

Scheme 4

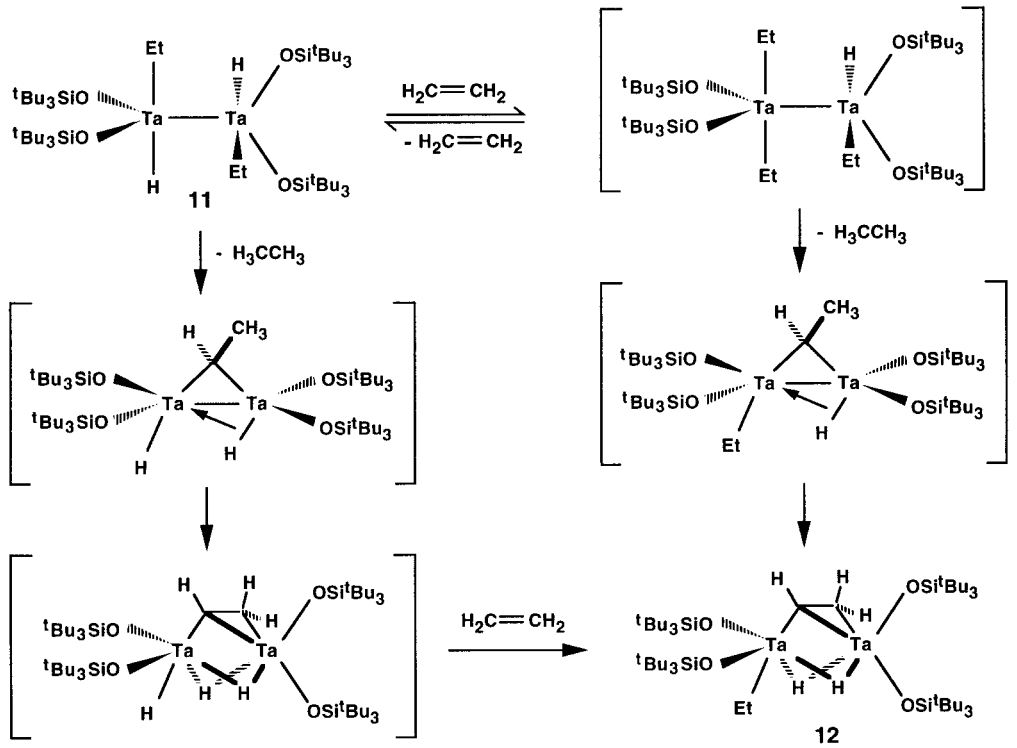

4. Ditantalum μ-Vinyl Formation. Given the stoichiometry requirements indicated by eq 11, the minor order in added ethylene on the rate of conversion of $[(silox)_2HTaEt]_2$ (**11**) to $[(silox)_2EtTa](\mu\text{-}CHCH_2)(\mu\text{-}H)_2[Ta(silox)_2]$ (**12**) is puzzling. The magnitude of k_H/k_D (~9) is most consistent with an α-abstraction[49] as the rate-determining step, but little else can be discerned mechanistically due to the aforementioned label scrambling problem. Scheme 4 illustrates a scenario whereby the α-abstraction can occur directly from **11** or from a triethylhydride−ditantalum complex generated via ethylene insertion. The former would not exhibit an order ($n = 0$) in $[C_2H_4]^n$, while the latter would ($n = 1$), thereby providing a possible explanation for the observations. β-H-eliminations from the μ-ethylidenes lead to **12**, although some formal rearrangement of the ditantalum bond and hydride is a necessary accompaniment. Any post-abstraction involvement of ethylene should have no consequence on its order, unless the α-abstraction is reversible, which is improbable. It is somewhat surprising that further ethane loss to give a ditantalum analogue of $[(silox)_2W]_2(\mu\text{-}CH)(\mu\text{-}CH_2)(H)$ (**9**), or loss of both C_2H_6 and H_2 leading to "$[(silox)_2Ta]_2(\mu{:}\eta^2,\eta^2\text{-}HCCH)$", or especially "$[(silox)_2Ta]_2(\mu\text{-}CH_2)_2$", was not cleanly observed. The μ-vinyl dihydride **12** does decompose, but the identification of any one of the myriad products has proven difficult.

Conclusions

Just as the steric bulk of the silox ligand proved crucial in synthesizing the first isolable $(W{\equiv}W)^{6+}$ di-

(49) Slaughter, L. M.; Wolczanski, P. T.; Klinckman, T. R.; Cundari, T. R. *J. Am. Chem. Soc.* **2000**, *122*, 7953−7975.

hydride,[30] it has also permitted preparation of μ:η^2-alkyne dihydrides, $[(silox)_2W]_2(\mu{:}\eta^2,\eta^2\text{-RCCR}')(\mu\text{-H})_2$ (R = R′ = H, **2a**; CH_3, **2b**; R = H, R′ = Ph, **2c**), in the absence of additional donor ligands. While the alkyne adducts **2a**−**c** resemble known $(RO)_6W_2(\mu{:}\eta^2\text{-}C_2R'_2)(py)_x$ species,[4,9] few analogues of their degradation products, $[(silox)_2W]_2(\mu\text{-CR})(\mu\text{-CR}')$ (R = R′ = H, **4a**; CH_3, **4b**; R = H, R′ = Ph, **4c**), have been found. $(^tBuO)_4W_2(\mu\text{-CPh})_2$ remains the lone related complex,[6] presumably due to its unusual high-temperature formation and the difficulty of achieving alkoxide eliminations from the most likely precursors, $(RO)_6W_2$.

The room-temperature dehydrogenation and carbon−carbon bond cleavage of ethylene, promoted by reduction of $[(silox)_2WCl]_2$ (**3**), is a unique event whose ultimate product, $[(silox)_2W]_2(\mu\text{-CH})_2$ (**4a**), presumably reflects the favorable thermodynamics of the $W_2(\mu\text{-CH})_2$ core formation. Precedent for the CH activation is clear from Messerle's work,[41] but the actual C−C cleavage event leading to $[(silox)_2W]_2(\mu\text{-CH})(\mu\text{-CH}_2)(H)$ (**9**)—certain from the absence of a $^{13}C-^{13}C$ coupling constant when $^{13}C_2H_4$ was used—is rare in early transition metal chemistry.

While the abstraction events responsible for the conversion of $[(silox)_2W(CH_2CH_3)]_2$ (**5**) to $[(silox)_2W]_2(\mu\text{-CMe})_2$ (**4b**) have ample precedent[17,18,44−48] and the favorable thermodynamics of bis-μ-alkylidyne formation are unquestionable,[16−28] analogous ditantalum chemistry was not found. In the decomposition of $[(silox)_2EtTa](\mu\text{-CHCH}_2)(\mu\text{-H})_2[Ta(silox)_2]$ (**12**), "$[(silox)_2Ta]_2(\mu\text{-CH})_2$" was anticipated as the most likely product. It is certainly conceivable in view of previous calculations on $(RO)_4W_2(\mu\text{-CR}')_2$[25] that the additional electrons in metal−metal bonding orbitals play a critical role in the stability of the $M_2(\mu\text{-CR})_2$ framework. Two less electrons in the ditantalum system indicate that prior reduction of one or both metal centers must occur if the μ-vinyl ligand of **12** was to be cleaved; alternatively, additional abstraction events—such as loss of ethane from **12** to afford "$[(silox)_2Ta]_2(\mu{:}\eta^2,\eta^2\text{-HCCH})(\mu\text{-H})_2$"—must occur to provide a ready path for CC bond cleavage. In any case, no clean version of these events was noted, and the commonality hoped for in the study of the ditantalum system proved to be modest.

Experimental Section

General Considerations. All manipulations were performed using either glovebox or high vacuum line techniques. Hydrocarbon solvents containing 1−2 mL of added tetraglyme and ethereal solvents were distilled under nitrogen from purple benzophenone ketyl and vacuum transferred from the same prior to use. Benzene-d_6 was dried over activated 4 Å molecular sieves, vacuum transferred, and stored under N_2; toluene-d_8, methylcyclohexane-d_{14}, and THF-d_8 were dried over sodium benzophenone ketyl. All glassware was oven dried, and NMR tubes were additionally flamed under dynamic vacuum. Ethylene, 2-butyne, acetylene (Matheson), and $^{13}C_2H_4$ (Cambridge) were used as received. H_2 and D_2 were passed over activated MnO and 4 Å sieves. $[(silox)_2WH]_2$ (**1**), $[(silox)_2WMe]_2$, $[(silox)_2WCl]_2$ (**3**), $[(silox)_2WEt]_2$ (**5**),[30] and $[(silox)_2TaH_2]_2$ (**10**)[38] were prepared according to published procedures.

NMR spectra were obtained using Varian XL-200, XL-400, and VXR-400S and Bruker AF-300 spectrometers. Chemical shifts are reported relative to TMS. Infrared spectra were recorded on a Mattson FT-IR interfaced to an AT&T PC7300 computer or on a Perkin-Elmer 299B spectrophotometer. Elemental analyses were performed by Texas Analytical Laboratories, Houston, TX, Oneida Research Services, Whitesboro, NY, and Robertson Microlit Laboratories, Madison, NJ.

Procedures. 1. $[(silox)_2W]_2(\mu{:}\eta^2,\eta^2\text{-HCCH})(\mu\text{-H})_2$ (2a). A flask containing **1** (100 mg, 0.081 mmol) in 8 mL of hexanes was cooled to −78 °C, and acetylene (121 Torr, 0.081 mmol) was admitted via a 12.3 mL calibrated gas bulb. The light brown solution darkened immediately. After warming to 25 °C and stirring for 2 h, the solvent was removed in vacuo, giving a red-orange crystalline solid that was used without further purification. ^1H NMR analysis indicated >95% conversion to **2a**.

2. $[(silox)_2W]_2(\mu{:}\eta^2,\eta^2\text{-MeCCMe})(\mu\text{-H})_2$ (2b). An NMR tube charged with **1** (50 mg, 0.041 mmol) was attached to a needle valve adapter. C_6D_6 (0.6 mL) was vacuum distilled into the tube, then 2-butyne (15 Torr, 0.041 mmol) was admitted via a calibrated 50.1 mL gas bulb. Partial conversion (20%) to **2b** was observed after 15 min at 25 °C. The reaction was complete after 4 h, yielding a solution of brown **2b** in 95% conversion. IR (Nujol): $\nu(W_2H/D) = 1522/1145\ cm^{-1}$.

3. $[(silox)_2W]_2(\mu{:}\eta^2,\eta^2\text{-HCCPh})(\mu\text{-H})_2$ (2c). To a solution of **1** (50 mg, 0.041 mmol) in C_6D_6 (0.6 mL) was added phenylacetylene (4.5 μL, 0.041 mmol) via a microliter syringe. The solution was transferred into an NMR tube attached to a needle valve adapter, freeze−pump−thaw degassed, and flame-sealed under vacuum at 77 K. Conversion to **2c** was complete (90% yield by ^1H NMR) after 8 h at 25 °C.

4. $[(silox)_2W]_2(\mu\text{-CH})_2$ (4a). a. From 2a. Into an NMR tube charged with **2a** (50 mg, 0.040 mmol) was vacuum-distilled 0.6 mL of C_6D_6. The tube was cooled to 77 K and flame-sealed under vacuum. Thermolysis in an 80 °C bath for 5 h produced H_2 and **4a**, which was isolated as a flocculent yellow solid by vacuum filtration (33 mg, 66%).

b. Reduction of 3 with C_2H_4. Into a glass bomb reactor containing $[(silox)_2ClW]_2$ (**3**, 250 mg, 0.192 mmol) and 0.9% Na/Hg (1.00 g, 0.391 mmol) was vacuum-distilled 5 mL of DME. The solution was freeze−pump−thaw degassed and cooled to −78 °C. C_2H_4 (~12 mmol) was admitted from a 300 mL vacuum manifold. The solution was warmed to 25 °C and stirred vigorously for 30 min, as a yellow precipitate formed. The bomb was degassed via Toepler pump, and the volatiles were passed through three liquid nitrogen traps and collected in a 16 mL volume (174 Torr, 0.151 mmol). The gas was converted quantitatively to H_2O by circulation over CuO (300 °C), indicating evolution of 0.79 equiv of H_2. The yellow solid residue was extracted from the salts by repeated washing with hexanes. Concentration of the resulting yellow solution to 1 mL, filtration, and drying in vacuo yielded 163 mg of yellow solid **4a** (68% yield). Anal. Calcd for $W_2Si_4O_4C_{50}H_{110}$: C, 47.84; H, 8.83. Found: C, 47.21; H, 8.60.

5. $[(silox)_2W]_2(\mu\text{-CMe})_2$ (4b). a. From 2b. A C_6D_6 solution of freshly prepared **2b** (54 mg, 0.041 mmol) in a sealed NMR tube was heated at 120 °C and monitored periodically by ^1H NMR spectroscopy. The solution turned yellow over the course of 6−7 h as **4b** formed in >95% conversion. H_2 was detected in the ^1H NMR spectrum. The NMR tube was cracked open inside an evacuated flask, and the volatiles were passed through three liquid nitrogen traps and collected (16 mL) via Toepler pump (21 Torr, 0.018 mmol, 0.45 equiv). The yellow crystals of **2b** were washed with 0.5 mL of benzene, collected, and dried via vacuum filtration (29 mg, 58% yield).

b. From $[(silox)_2WEt]_2$ (5). A solution of **5** (50 mg, 0.040 mmol) in 0.6 mL of C_6D_6 was loaded into an NMR tube. The solution was freeze−pump−thaw degassed three times, and ethylene (100 Torr, 0.27 mmol) was condensed into the tube at 77 K via a 50.1 mL gas bulb. The tube was flame-sealed, then heated to 100 °C for 2 h. Upon cooling to 25 °C, yellow crystals precipitated. ^1H NMR analysis of the supernatant showed quantitative formation of **4a** and evolution of ethane. The tube was cracked open, and yellow crystals of **4a** were collected and dried by vacuum filtration (34 mg, 68% yield).

6. [(silox)$_2$W]$_2$(μ-CH)(μ-CPh) (4c). A C_6D_6 solution of freshly prepared **2c** (54 mg, 0.041 mmol) in a sealed NMR tube was heated at 120 °C. Periodic ^{1}H NMR monitoring revealed quantitative conversion to **4c** and release of H_2 after 8 h thermolysis. Cooling the solution to room temperature yielded orange crystals, which were isolated and dried by vacuum filtration (23 mg, 43% yield).

7. [(silox)$_2$W]$_2$(μ:η^2,η^2-H$_3$CC≡CCH$_3$) (8). a. Synthesis and Conversion to 4b. Into a flask containing **3** (75 mg, 0.058 mmol) and 0.9% Na/Hg amalgam (296 mg, 0.116 mmol Na) at 77 K was distilled 3 mL of DME. 2-Butyne (400 Torr, 13 mmol) was admitted from a 600 mL vacuum manifold, then the solution was warmed to 25 °C and stirred for 1.5 h. Volatiles were removed in vacuo, and the brown residue was triturated with 1 mL of benzene, then redissolved in 1 mL of C_6D_6. An aliquot was loaded into an NMR tube attached to a needle valve adapter and freeze−pump−thaw degassed, and the tube flame-sealed under vacuum. ^{1}NMR analysis indicated a 70% yield of **8**, contaminated with 30% (silox)$_2$HW≡W(OSi^{t}Bu$_2$-CMe$_2$CH$_2$)(silox) (**6**). Thermolysis of this solution for 5 h at 80 °C converted **8** quantitatively to **4b**.

b. Conversion to 2b. The remaining C_6D_6 solution of **8** (with **6**) from above was loaded into an NMR tube attached to a needle valve adapter. The solution was freeze−pump−thaw degassed three times and frozen at 77 K. H_2 (700 Torr) was admitted and the tube flame-sealed. ^{1}H NMR analysis showed a 70:30 ratio of **2b** and **1**. Thermolysis of this solution for 20 h at 110 °C showed <20% conversion to **4b** by ^{1}H NMR spectroscopy. A similar procedure using D_2 gas yielded **2b**-d_2 for IR analysis.

8. [(silox)$_2$W](μ-CH)(μ-CH$_2$)(μ-H) (9). A 5 mL flask charged with **3** (50 mg, 0.038 mmol) and 0.9% Na/Hg (194 mg, 0.076 mmol Na) was attached to a needle valve adapter equipped with a sidearm leading to an NMR tube. THF-d_8 (0.75 mL) was distilled into the evacuated flask at 77 K, then an excess of ethylene (150 Torr, 4.9 mmol) was admitted to a 600 mL manifold and condensed into the flask. The solution was warmed to 25 °C and stirred vigorously. An intense red color developed within 5 min, whereupon the solution was rapidly cooled to −78 °C and stirred under dynamic vacuum for 1 min to degas. The sidearm and NMR tube surfaces were cooled to −78 °C, and the solution was rapidly decanted into the NMR tube. The tube was cooled to 77 K for flame-sealing and kept frozen until just before inserting into a precooled probe for ^{1}H NMR analysis. A similar procedure using $^{13}C_2H_4$ generated **9**-$^{13}C_2$ for NMR analysis.

9. [(silox)$_2$HTaEt]$_2$ (11). A 25 mL flask charged with 0.150 g (0.123 mmol) of [(silox)$_2$TaH$_2$]$_2$ (**10**) was attached to a gas bulb and mounted on the vacuum line. At −78 °C, 10 mL of diethyl ether were distilled in, and 2 equiv of ethylene was admitted via the gas bulb. The solution turned dark brown and was stirred for 15 min. The solvent was removed, affording a brown solid. ^{1}H NMR spectroscopic analysis indicated a 3:1 mixture of **11** and **12**.

10. [(silox)$_2$EtTa](μ-CHCH$_2$)(μ-H)$_2$[Ta(silox)$_2$] (12). To a 25 mL flask charged with 0.200 g (0.163 mmol) of **10** was vacuum distilled 10 mL of benzene at −78 °C. The solution was exposed to 1 atm of ethylene, resulting in a dark brown color that became deep orange upon warming to 25 °C during the course of 12 h. The benzene was removed, and the dark orange solid was triturated with three 8 mL portions of hexanes and filtered. Upon reducing the volume to 2 mL and cooling to −78 °C, 0.114 g of **12** was isolated by filtration (56%).

X-ray Crystallographic Studies. 11. Single-Crystal X-ray Diffraction Analysis of [(silox)$_2$W]$_2$(μ-CCH$_3$)$_2$ (4b). A yellow block-shaped single crystal of **4b**, with dimensions 0.3 × 0.3 × 0.4 mm, was grown by cooling of a supersaturated benzene solution from 80 °C. The crystal was sealed in a Lindemann capillary for data collection at 298 K (Siemens R3m/V). Preliminary data collection and axial photographs indicated an orthorhombic lattice, and analysis of systematic absences indicated space group *Pbca*. Diffraction maxima were measured using variable speed ω-scans and graphite-monochromated Mo Kα radiation. After correction for Lorentz, polarization, background, and decomposition, 7572 (54.2%) of the unique data (13 962 out of 15 046 measured) were judged observed ($F > 4.0\sigma(F)$). The structure solution proceeded using direct methods and successive difference electron density maps (SHELXTL PLUS), full-matrix least-squares refinement was conducted with all non-hydrogen atoms anisotropic, and hydrogen atoms were treated as idealized contributions.

12. Single-Crystal X-ray Diffraction Analysis of [(silox)$_2$-EtTa](μ-CHCH$_2$)(μ-H)$_2$[Ta(silox)$_2$] (12). A crystal (0.30 × 0.20 × 0.05 mm) of **12** was immersed in polyisobutylene, extracted out with a glass fiber, and placed on the goniometer head of a Siemens SMART CCD area detector system equipped with a fine-focus molybdenum X-ray tube (λ = 0.71073 Å). Preliminary diffraction data revealed an orthorhombic crystal system. A hemisphere routine was used for data collection, determination of lattice constants, and identification of space group *Pbca*. A total of 55 978 reflections were collected, of which 8398 were symmetry independent (R_{int} = 0.0483). The data were processed with the Bruker SAINT program and corrected for absorption by SADABS. The structure was solved by direct methods (SHELXS), completed by subsequent difference Fourier syntheses, and refined by full-matrix least-squares procedures (SHELXL). Heavy atoms were refined with anisotropic displacement parameters, whereas all hydrogen atoms were included at calculated positions.

Acknowledgment. We thank the National Science Foundation (CHE-9528914) and Cornell University for support of this research.

Supporting Information Available: Crystal data, data collection, and solution and refinement details pertaining to [(silox)$_2$W]$_2$(μ-CCH$_3$)$_2$ (**4b**); CIF file pertaining to [(silox)$_2$EtTa]-(μ-CHCH$_2$)(μ-H)$_2$[Ta(silox)$_2$] (**12**). This material is available free of charge via the Internet at http://pubs.acs.org.

OM020037N